Journal of CO_2 Utilization 26 (2018) 380–387

Contents lists available at ScienceDirect

Journal of CO_2 Utilization

journal homepage: www.elsevier.com/locate/jcou

Sustainable packaging waste-derived activated carbon for carbon dioxide capture

Mohanad Idrees, Vijaya Rangari*, Shaik Jeelani

Department of Materials Science and Engineering, Tuskegee University, 1200 W Montgomery Rd, Tuskegee, AL 36088, United States

ARTICLE INFO

Keywords:
Carbon capture
Packaging waste
Activated carbon
Narrow micropores

ABSTRACT

Global greenhouse gases emissions have increased tremendously since 1950's due to excessive burning of fossil fuel. The objective of this work is to develop and investigate packaging waste-derived activated carbon for carbon capture. Activated carbon was synthesized by carbonization of peanut-shaped packaging waste followed by chemical activation using KOH at a ratio of one to four. The activated carbon was characterized for it is textural properties using N_2 adsorption at 77 K, and carbon dioxide adsorption isotherms at 273, 298 and 323 K. Non-Linear Density Functional Theory (NDLFT) was applied to carbon dioxide isotherm at 273 K to characterize narrow micropores and microporous structure of activated carbon. Field emission scanning electron microscopy (FE-SEM) and transmission electron microscopy (TEM) were used to investigate morphology and microstructure. TEM micrographs confirmed the existence of random micropores. We have also noticed that the textural properties were highly dependent on the concentration of the activating agent. Carbon dioxide adsorption on activated carbon materials has shown dependency on the volume of narrow micropores (less than 0.8 nm). The activated carbon materials have narrow micropore volume in a range of 0.155–0.292 cm^3, and BET surface area of 761–1383 m^2/g. Carbon activated with KOH ratio of three (WDC-03) has shown excellent CO_2 uptake of 5.33 and 4.24 mmol/g at 273 and 298 K respectively. Moreover, it has also shown a high value for the isosteric heat of adsorption (29.8–14.3 KJ/mol) and selectivity of ~16 over nitrogen.

1. Introduction

Among greenhouse gases, carbon dioxide (CO_2) is the major contributor to global warming and climate change. CO_2 comprised about 82% of the total US greenhouse gases (GHG) emissions in 2015 [1]. Its level has increased by 26.5% in the last 60 years. Without mitigation efforts to reduce emissions, the level is expected to increase by 200% by the end of this century; due to excessive burning of fossil fuels for power generation and other industrial processes [2]. Such practices will lead to catastrophic consequences including an increase in the earth's temperature, an increase of sea level and flooding of coastal areas. To counteract the danger of the elevated carbon dioxide level in the atmosphere, several capture and storage technologies were studied as potential methods to reduce the amount released to the environment [3–6].

Several technologies have proven effectiveness for carbon dioxide absorption and adsorption. For instance, the ethanolamines are widely used in industry for selective absorption of CO_2 from flue gases. This process is commonly used in industries which involve extensive use of carbon dioxide such as carbonated beverages industry [7]. However, this technology suffers from lack of sustainability and energy-intensive regeneration performed at temperature range of 100–120 °C. Furthermore, the corrosive nature of ethanolamines reduce the service life of process equipment [8,9]. Adsorption of CO_2 through vacuum swing adsorption process is proposed to be an excellent alternative for conventional ethanolamine absorption technology. The major advantages of adsorption process are sustainability, wide range of available adsorbents and mild regeneration temperature. Various materials such as zeolite, silica, metal organic frameworks (MOF) and activated carbon have been used as adsorbents [10–12]. Recently, the demand for efficient and green materials for water wastewaters treatment has been increasing. This demand resulted in the development of efficient adsorbents from different materials, such as carbon nanotubes, metal oxides nanoparticles, and waste biomass. The adsorbents have shown excellent performance in the removal of pollutants such as hazardous dyes and heavy metals from wastewaters [13–28].

Activated carbon has several advantages over other adsorbents. It has excellent regeneration stability in the humid environment over zeolite and MOF, low cost, wide range available sources and activation processes for its production [29–32]. The most important feature of

* Corresponding author.
E-mail address: vrangari@tuskegee.edu (V. Rangari).

https://doi.org/10.1016/j.jcou.2018.05.016
Received 7 March 2018; Received in revised form 14 May 2018; Accepted 16 May 2018

activated carbon is its easily tailorable properties by varying the type and amount activating agent and/ activation condition to produce the desirable textural properties such as surface area, pore volume, pore size, and pores size distribution [33–38]. Moderate KOH to carbon ratio (2–3) produces a high narrow micropore volume, which is responsible for carbon dioxide adsorption. The wheat flour-derived activated carbon using KOH ratio of three showed improved CO_2 adsorption of 5.70 and 3.48 mmol/g at 273 and 298 K, respectively [39]. Sawdust activated carbon synthesized using KOH ratio of two and moderate activation temperature of 600 °C showed high CO_2 adsorption capacity of 4.8 mmol/g at 298 K [32]. Previous studies have correlated the CO_2 adsorption on activated carbon to the volume of ultra or narrow micropores with size less than 0.8 nm and concluded that it is the major contributor to CO_2 uptake [40]. Moreover, studies on utilization of chemicals to produce nitrogen-doped activated carbon concluded that nitrogen content improves carbon dioxide uptake at elevated temperature as well as enhancing cyclic stability [41,42].

Although activated carbon from various waste and biomass sources such as waste coffee ground, pine nutshell, granular bamboo and potato starch-were investigated for carbon capture, there are plenty of potential waste materials to be explored [43–46]. A Recent survey shows that the significant quantities of packaging waste disposed in landfills resulted in increased environmental concerns [47]. Strategies such as recycling, reuse, as well as the conversion of waste to value-added char are currently employed to reduce the large quantities disposed to landfills. One of the well-known methods, of converting waste to value-added char is heating it at elevated temperatures in an inert environment and followed by activation. This method was found to be helpful in minimizing the impacts and reducing the disposed amounts [48,49]. Although produced pyrolytic char is energy-rich, it has poor textural properties in terms of BET surface area and pore volume [50] which limits its utilization; chemical activation can highly improve char properties.

In this work, we explored the packaging waste as a sustainable source for production of activated carbon with excellent CO_2 capture capabilities and CO_2/ N_2 selectivity, using varying amounts of KOH and moderate synthesis temperature. To the best of our knowledge, this is the first report of a study that involves using (BRAN FOAM TOP) peanut shaped packaging waste to produce activated carbon for CO_2 Capture.

2. Materials and methods

2.1. Materials

Peanut shaped loose filler packaging material (BRAN FOAM TOP), made primarily from starch, was procured from ECOLOPACK (Japan). Potassium hydroxide KOH was purchased from Sigma-Aldrich.

2.2. Synthesis

Peanut shaped packaging waste (PSPW) was first washed with distilled water and allowed to dry in an oven overnight at 120 °C. Dried (PSPW) was ground into a fine powder in a ceramic mortar, and then the powder was carbonized in a furnace tube under the flow of nitrogen at a heating rate of 5 °C/min from room temperature to 500 °C. The sample was kept at 500 °C for one hour and then allowed it to cool. The resulting carbonized waste (CW) was mixed with potassium hydroxide KOH at ratios of 1, 2, 3 and 4 by weight. The CW and KOH mixtures were stirred for 3 h at 65 °C and vacuum dried at 120 °C overnight. The dried CW / KOH mixtures were placed in ceramic muffle and heated in a tube furnace at a heating rate of 5 °C/min from room temperature to 700 °C and kept at 700 °C for one hour. After cooling, the products were washed with dilute HCl and distilled water several times until neutral pH is achieved. The synthesized activated carbon was vacuum dried at 120 °C overnight. Samples were labeled based on KOH ratio WDC-0X where X stands for KOH ratio.

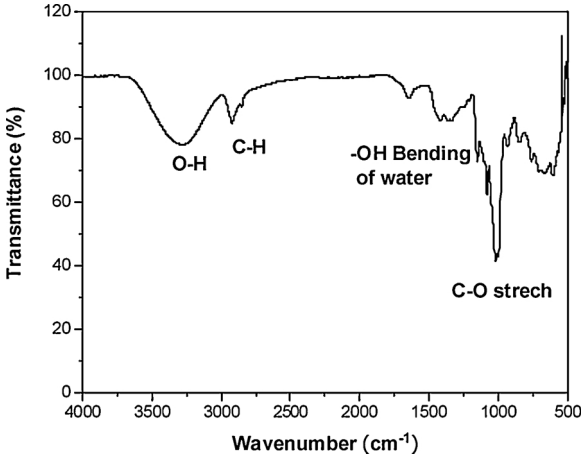

Fig. 1. FTIR spectrum of pristine packaging waste.

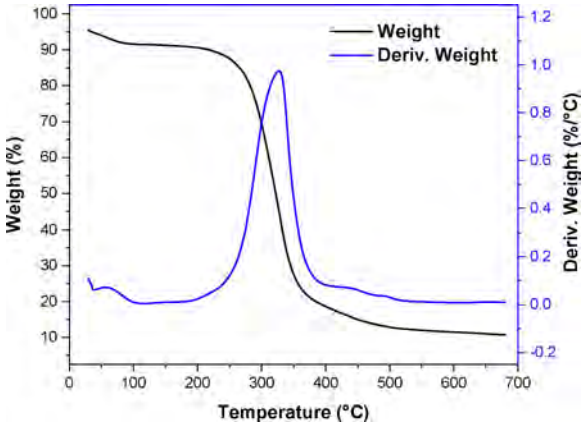

Fig. 2. Pyrolysis of pristine packaging waste under the flow of nitrogen.

3. Characterization

3.1. Pristine packaging waste (PSPW)

3.1.1. Chemical structure

The chemical structure of pristine packaging waste was determined using Fourier-transform infrared spectroscopy (FTIR) Shimadzu FTIR 8400 s machine equipped with MIRacle TM ATR was used to obtain spectrum in the range of 500-4000 cm^{-1}.

3.1.2. Thermal properties

Thermogravimetric analysis (TGA) of pristine packaging waste was carried out in TA Q 500TGA. PSPW (15 mg) samples were heated from room temperature to 700 °C at a heating rate of 5 °C/ min, under nitrogen environment.

3.2. Surface morphology and microstructure

The morphology and microstructure of CW and activated Carbon materials were investigated using FE-SEM (Jeol JSM −7200 F) and Transmission Electron Microscope (TEM-Jeol 2010).

3.3. Nitrogen adsorption

Textural properties were investigated using NOVA2200e (Quantachrome, USA) surface area and pore size analyzer. All samples were vacuum degassed at 150 °C overnight to remove volatiles and used for characterization. Nitrogen adsorption-desorption isotherms were obtained at 77 K and a partial pressure range of (0.005–0.99),

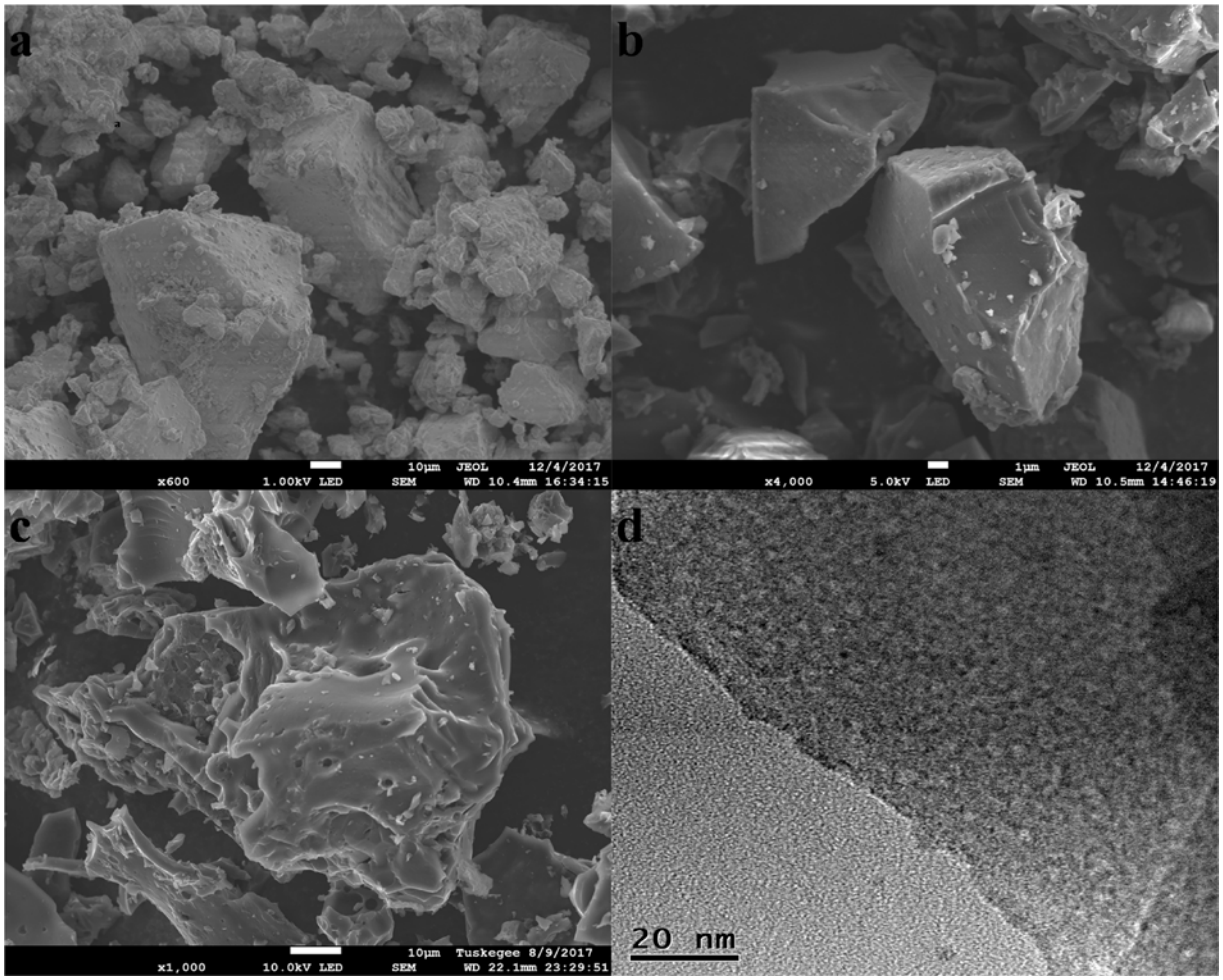

Fig. 3. Morphology and microstructure of carbonized waste and activated carbon (a) SEM micrograph of packaging waste (PSWP), (b) SEM micrograph of carbonized waste (CW), (c) SEM micrograph of activated carbon (WDC-03), (d) TEM micrograph of WDC-03.

adsorption-desorption isotherms were further used for estimation of BET surface area, pore volume, and pore size distribution. BET surface area was calculated using multi-point test in a partial pressure range of (0.05–0.3), micropore volume was estimated using Non-Linear Density Functional Theory (NDLFT). Total pore volume was measured at a partial pressure of 0.99. Mesopore volume was calculated as the difference of total pore volume at 0.99 and micropore volume.

3.4. Narrow micropore and carbon dioxide adsorption

Nonlinear density functional theory (NDLFT) was used to measure the narrow micropores in the range of (0.32–0.8 nm) from carbon dioxide adsorption isotherm at 273 K. The saturation vapor pressure was changed in NovaWin Qunatachrome software to (26,140 mmHg) which correspond to CO_2 at 273 K. CO_2 adsorption was investigated by measuring adsorption isotherms at different temperatures (273, 298 and 323 K) using NOVA2200e (Quantachrome, USA). A recirculation dewar filled with water/antifreeze mixture and connected to chiller was used to maintain bath temperature at the desired setpoint. Both the activated carbon textural properties and carbon dioxide adsorption values were reproducible with a very slight variance.

4. Results and discussion

4.1. Chemical structure

Fig. 1 shows FTIR spectrum of peanut-shaped pristine packaging waste (PSPW). The broad transmission band around 3315 cm^{-1} is ascribed to OH stretching. The peak around 2920 cm^{-1} is attributed to CH stretching. The small hump at 1640 cm^{-1} corresponds to OH bending of water. The bands around 1040 and 1100 are assigned to C–O stretching on the polysaccharide. All the peaks on packaging waste FTIR spectrum are typical cellulose peaks. Our FTIR spectrum is similar to previous spectra reported in [51,52].This finding proved for us that the major constituent of packaging waste was starch.

To determine the pattern of packaging waste decomposition TGA was carried out, Fig. 2. represents the pyrolysis of the pristine packaging (PSPW) waste. A slight decrease in weight in the range of 35–100 °C was observed due to the removal of moisture content. The most of the weight loss occurs between 250 and 400 °C, corresponds to the decomposition of volatiles in the waste. Derivative weight graph shows maximum degradation rate around 330 °C due to the decomposition of cellulose. The slight and progressive mass loss, between 400 and 700 °C, is ascribed to the char consolidation.

4.2. Morphology and microstructure

Pristine Packaging waste morphology is shown in Fig. 3(a) big flakes with an irregular form and size of (20–30 µm). Fig. 3(b) shows CW. It shows flakes with a flat and uniform surface similar to PSWP. The size of particles is reduced due to materials loss during carbonization. Fig. 3(c), represents WDC-03. KOH activation has led to etching of surface and formation of visible pores with a diameter of around one µm and slight shrinkage in carbon particle size. The effective pores are

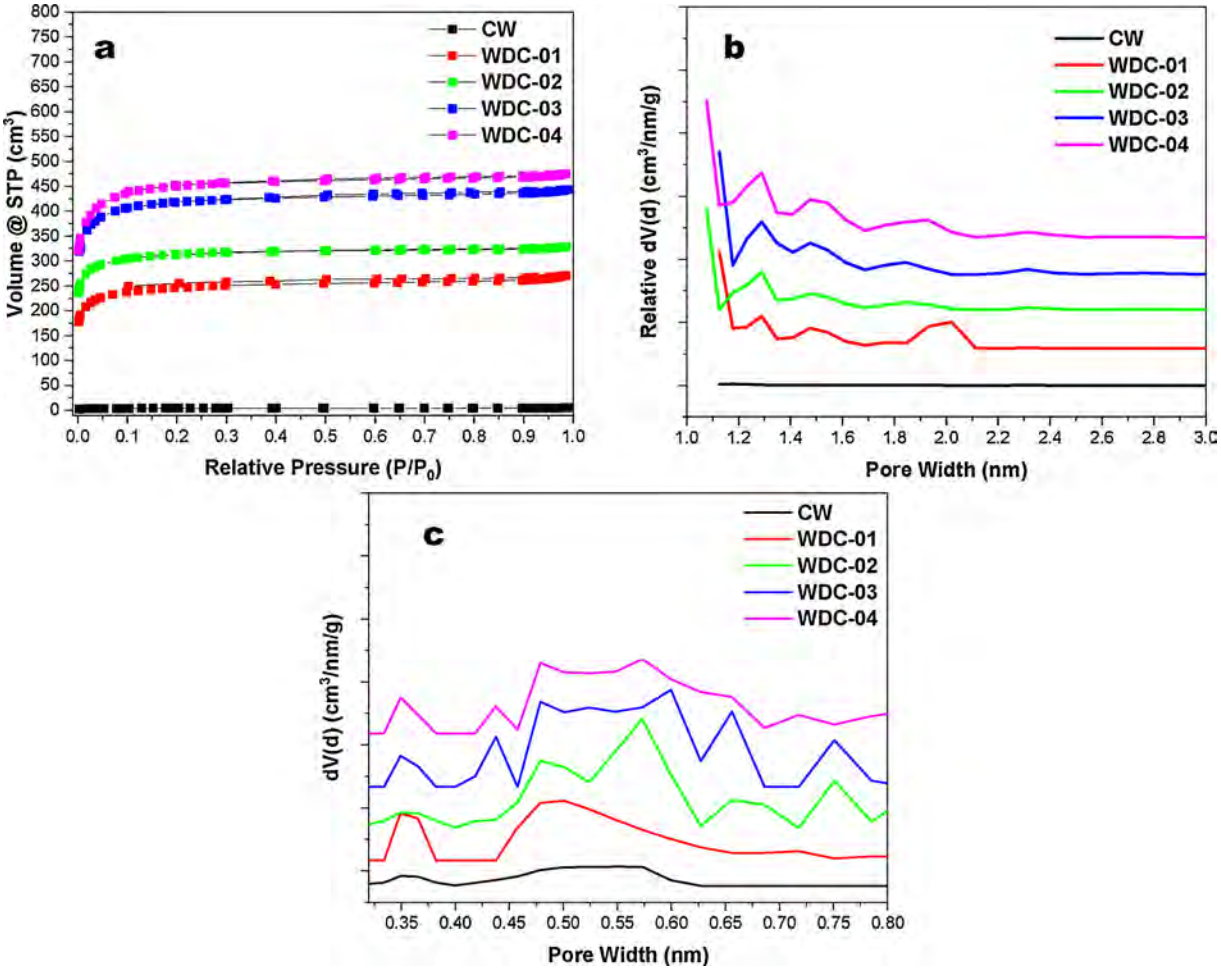

Fig. 4. Textural Properties (a) Nitrogen adsorption-desorption isotherm for carbonized waste and activated carbon materials, (b) Pore size distribution, (c) Narrow micropore size distribution.

Table 1
Summary of textural properties and carbon dioxide uptake.

	S_{BET} (m^2/g)	$V_{0.8}$ (cm^3)	V_m (cm^3)	V_{Mes} (cm^3)	V_T (cm^3)	CO_2 UPTAKE		
						273 K	298 K	323 K
CW	12.1	0.050	0.065	0.015	0.080	0.88	0.70	0.47
WDC-01	761	0.155	0.363	0.056	0.4189	3.04	2.41	0.88
WDC-02	963	0.245	0.439	0.069	0.508	4.73	3.10	1.05
WDC-03	1283	0.292	0.582	0.104	0.686	5.33	4.24	1.21
WDC-04	1383	0.234	0.633	0.103	0.736	4.50	3.93	1.18

narrow, and it was difficult to measure the pores sizes in SEM micrographs. TEM gave a better insight of activated carbon microstructure. Fig. 3(d) shows randomly distributed micropores, demonstrating the microporous structure of the activated carbon material.

4.3. Nitrogen adsorption and pore size distributions

Fig. 4(a) shows full adsorption desorption isotherms. All isotherms presented are type I according to IUPAC classification in which the amount of adsorbed gas at a relative pressure higher than 0.1 remains constant or increases very slightly. These results indicate the carbon materials are highly microporous [53]. Table 1 summarizes the textural properties of packaging waste-derived carbon materials. KOH activation has dramatically increased nitrogen adsorption, which indicated an increase in both the surface area and pores volume. (CW) has a very low BET surface area of 12.1 m^2/g and poor pore volume; KOH activation has improved the textural properties even at lower ratios. WDC-01 corresponding to activated carbon with KOH ratio of one led to around 70 folds' increase in surface area and five times increase in total pore volume. Both BET surface area and pore volume increased as the ratio of the activating agent increased, indicating a giant increase in the number of pores. WDC-04 has the highest surface area and pore volume among other samples with a surface area of 1383 m^2/g and pore volume of 0.736 cm^3.

Pore size distribution was obtained from the nitrogen isotherm using NDLFT nonlinear density functional theory-assuming slit pores. Fig. 4(b) shows the pore size distribution of CW and activated carbon materials. The distribution followed the same pattern for all samples, a slight portion of pores have size around 2–2.5 nm with a peak at 2.25 while the rest of the pore sizes were less than 2.0 nm confirming the microporous nature of carbon materials. The pores with size less than 2.0 nm were distributed around 1.25, 1.5 and 1.75–2.0 nm, but most of them were distributed around 1.25 nm. Pore size distribution obtained from nitrogen isotherm, as in Fig. 4(b) shows the quantification of micropores with size greater than one nanometer as well as mesopores. For the purpose of carbon dioxide adsorption, the volume of narrow micropores (less than 0.8 nm) is of great importance. Carbon dioxide adsorption mainly happens in narrow micropores. Van der Waals forces from the wall of narrow micropores facilitate interaction between carbon dioxide molecules and the surface of activated carbon and improve carbon dioxide adsorption. The overlapping of the potential energy field due the walls of narrow micropores results in an improved potential field in favor of adsorption [53,54]. Moreover, carbon dioxide

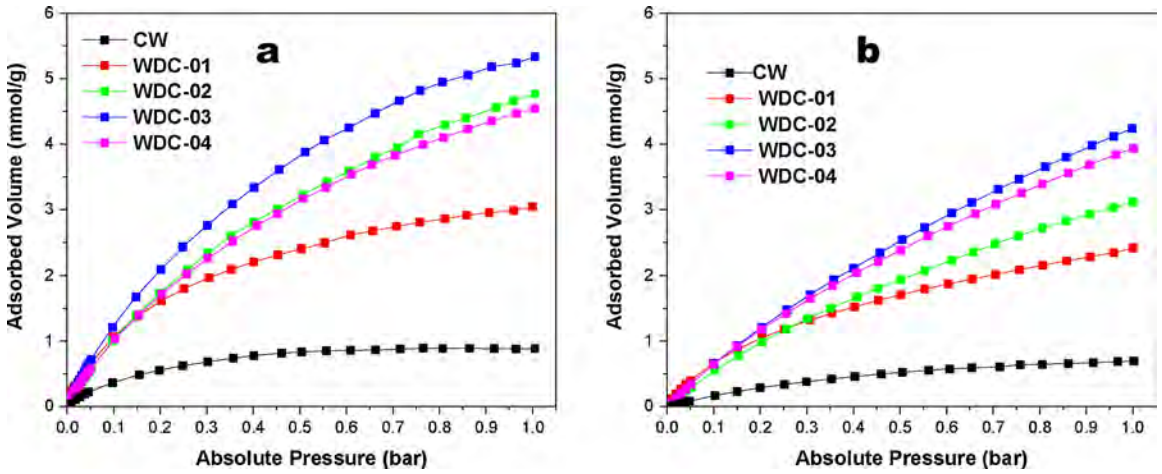

Fig. 5. Carbon dioxide adsorption on carbonized waste and activated carbon materials (a) adsorption at 273 K, (b) adsorption at 298 K.

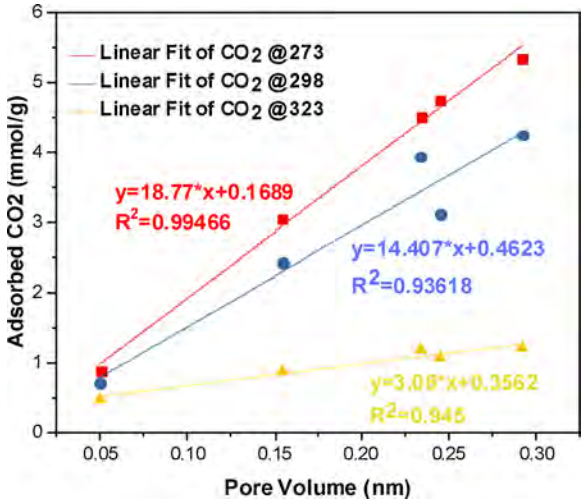

Fig. 6. Correlation between the volume of narrow micropore and carbon dioxide uptake at 273, 298 and 323 K.

isotherm at 273 K has been suggested to provide an accurate and efficient evaluation of volume and distribution of pores in the range of (0.32–1.5 nm) [53].

Interestingly, the volume of narrow micropores did not follow the same pattern of micropores, increasing with increasing the amount of KOH. It followed the law of diminishing returns or limiting factor, where amount the ratio of KOH is the limiting factor. With KOH ratios of 1, 2 and 3, the volume increased with KOH ratio. WDC-03 has the highest narrow micropore volume of 0.292 cm^3. As the KOH ratio is increased to 4, corresponding to WDC-04, the narrow micropore volume decrease to 0.234 cm^3.

(CW) has poor narrow micropore volume of 0.05 cm^3, as shown in Fig. 4(c) the pore sizes distributed around 0.35 and 0.45–0.60 nm. Although activated carbon materials show pores distributed around 0.35, 0.45 and 0.65 nm most of the pores were distributes in the range 0.45–0.65 nm as shown in Fig. 4(c). During the activation process, as KOH etches the carbon surface, it creates more pores and enhances the volume of already existing ones. Only, WDC-03 shows a portion of pores with size around 0.75 nm contributing to narrow pore volume. This may justify its excellent carbon dioxide adsorption performance.

In general, textural properties (BET surface area, pore volume, and micropore volume) have initially ramped with KOH activation and then showed increase proportional to activating agent ratio as shown in Table 1. Narrow micropore volume followed the same trend in the beginning. However, it dropped when KOH ratio is greater than three. Pore size distribution obtained from N_2 and CO_2 isotherms confirmed the microporous structure of activated carbon. In addition to, the presence of substantial amount of narrow micropores.

4.4. Carbon capture

As profiled in Table 1 and Fig. 5, carbon dioxide adsorption of (CW) was less than 1.0 mmol/g at 273 K and 1.0 bar. At 273 K, all activated carbon samples show increased carbon dioxide uptake with increasing KOH ratio in the range of 1–3 with figures of 3.0–5.3 mmol/g. WDC-04 has considerably high uptake of 4.5 mmol/g. However, it is lower than CO_2 adsorption of WDC-03. This is due to drop of narrow micropore volume at high KOH ratios. Carbon dioxide adsorption at 298 K shown in Fig. 5(b) and it shows a similar trend as (a), KOH ratio of one has increased the amount adsorbed from 0.7 to 2.4 mmol/g. Similar to Fig. 5(a) WDC-03 has the highest uptake of 4.2 mmol/g as the ratio of KOH is increased to 4 it dropped to 3.9 mmol/g, this confirms the dependency of CO_2 adsorption on narrow microspore volume.

The uptake of CO_2 at 273, 298 and 323 K was correlated with narrow micropore volume to obtain a good understanding of the effect of textural properties on carbon dioxide adsorption. Narrow micropore volume and amount of CO_2 adsorbed at different temperatures was plotted. The Linear fit tool was used to find the correlation between the adsorbed amount of CO_2 and narrow micropore volume at all temperature. As in Fig. 6, the results demonstrated an excellent linear fit for data with high R^2 values, greater than 0.90. These results are in good agreement with previously reported data, suggesting a strong relationship between the volume of the narrow pore and CO_2 adsorption [39,43,45].

Though all samples show substantial carbon dioxide uptake at all temperatures. WDC-03 has shown the best performance at 273 and 298 K with 5.3, 4.2 mmol/g respectively. As in Fig. 7(a), nitrogen adsorption on WDC-03 was also evaluated 298 K. It shows low figure even lower than CO_2 adsorption capacity at 323 K. This isotherm was later used for evaluation of selectivity of CO_2 over N_2.

4.5. Isosteric heat of adsorption

Fig. 7(b) shows Isosteric heat value of CO_2 adsorption on WDC-3. The values were calculated from WDC-03 adsorption isotherms at 273 and 298 K using Novawin software. The calculations were carried out according to Clausius–Clapeyron equation; Eq. (1) where Q_{st} is the isosteric heat of adsorption, R is the universal gas constant, θ is the adsorbed amount at a pressure p and temperature T. A plot of ln p vs. (1/T) results in line with a slope of $-Q_{st}/R$.

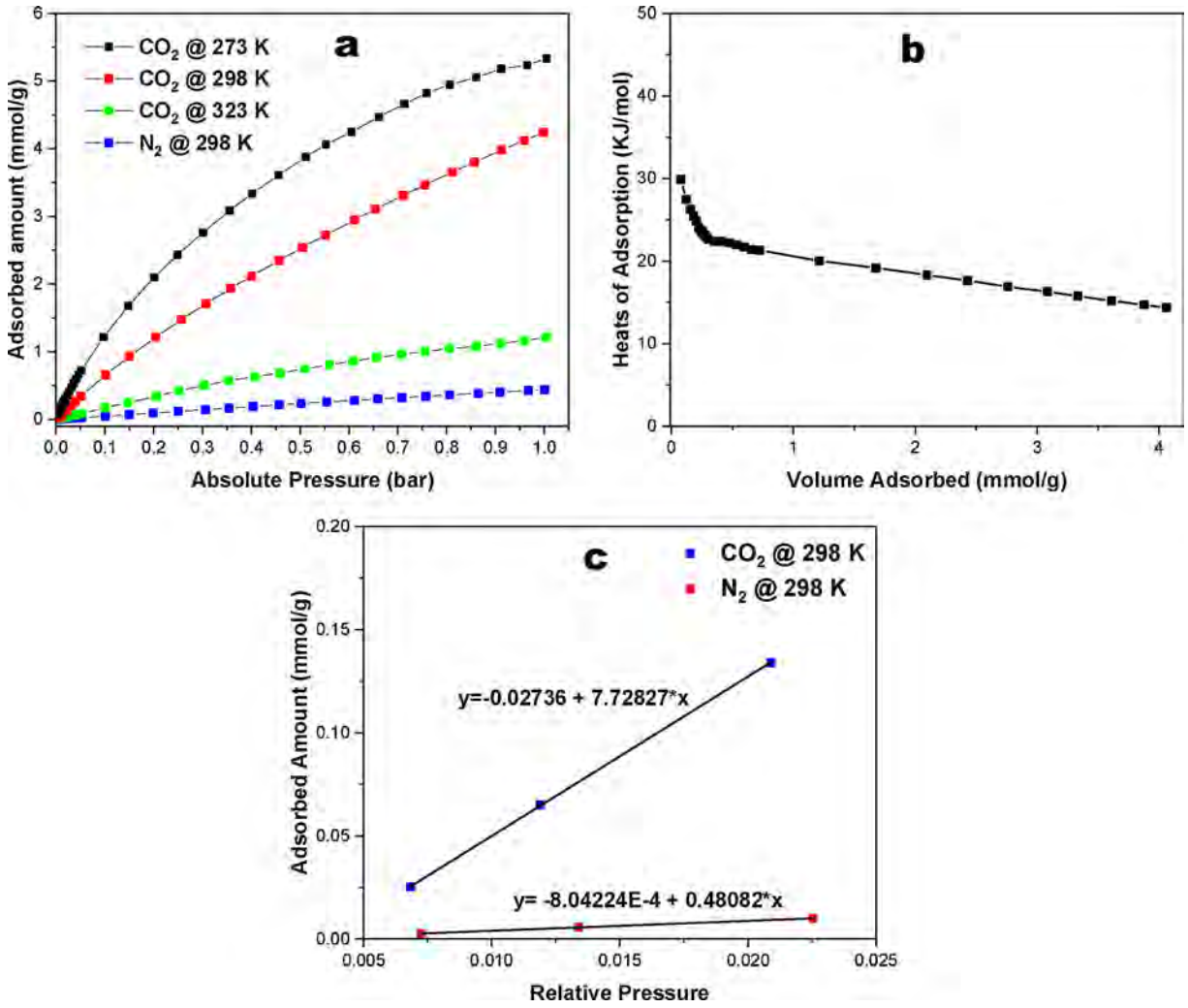

Fig. 7. Properties of activated carbon material (WDC-03), (a) Adsorption of carbon dioxide at different temperatures and N_2 at 298 K, (b) Isosteric heat of adsorption, (c) Henry's law initial slope for CO_2 and N_2 at 298 K for prediction of selectivity.

Table 2
Comparison of uptakes (298 K and 1.0 bar) for different porous carbon sorbents.

Sorbent	CO_2 Uptake (mmol/g)	Reference
waste longan shells	4.3	[55]
waste tobacco	2.5	[56]
waste Coca Cola®	1.97- 5.22	[57]
Spent coffee grounds	3	[31]
EFB biomass	3.71	[58]
Waste CDs and DVDs	3.3	[59]
Potato starch	3.5	[32]
Commercial Activated Carbon	2.46	[60]
CW	0.7	This work
WDC-01	2.4	This work
WDC-02	3.1	This work
WDC-03	4.2	This work
WDC-04	3.9	This work

$$-Q_{st} = R\left(\frac{\partial \ln p}{\partial\left(\frac{1}{T}\right)}\right)_\theta \quad (1)$$

The heat of adsorption value lies in the range of 29.8–14.3 KJ/mol, with the corresponding amount of adsorbed CO_2 in the range of 0.07–4.0 mmol/g. The initial heat of adsorption value, at low adsorbate loading (0.07 mmol/g), was as high as 29.8 KJ/ mole indicating a strong interaction between adsorbent and adsorbate. On the other hand, as the CO_2 loading increases to 4.0 mmol/g, the heat of adsorption value decreases to 14.3 KJ/ mole. This can be ascribed to filling of narrow micropore and weak interaction between the gas and activated carbon at higher loadings. The higher the initial value of the heat of adsorption at the lower gas loading leads to an improved selectivity for carbon dioxide over nitrogen [43].

4.6. Selectivity

The selectivity of CO_2 over N_2 for WDC-3 was evaluated by Henry's initial slope method. The first three points of both N_2 and CO_2 isotherms at 298 were plotted and fitted to a linear model as shown in Fig. 7(c). Henry's law initial slope method was used to calculate selectivity of CO_2 over N_2, and it was found to be 16.

Wasted derived activated carbon sample WDC-03 has a considerably high carbon dioxide uptake at 298 K and 1.0 bar. Table 2 compares adsorption capacity of different waste derived activated carbon as well as commercial ones. It can be concluded carbon dioxide uptake of WDC-03 at 298 is one of the best-reported values for activated carbon-derived from waste sources.

5. Conclusion

In conclusion, we have demonstrated facile synthesis of highly microporous activated carbon with excellent carbon capture performance,

using carbonization of highly abundant peanut shaped packaging waste followed by KOH activation and without application of template or nitrogen doping. The results show KOH activation has led to great improvement in textural properties. Activated carbon materials have considerably high BET surface area of 761–1383 m^2/g and total pore volume of 0.418–0.736 cm^3. The volume of narrow micropore, less than 0.8 nm, is greatly affected by the ratio of KOH in range of 1–3, and it drops with further increasing of KOH. The relationship between of narrow micropore volume and amount of adsorbed CO_2 has shown good linear fit at different temperatures, which confirms that adsorption of CO_2 mainly happens on narrow micropores. KOH carbon ratio of (3:1) corresponds to WDC-3 resulted in the highest narrow micropore volume and the best CO_2 adsorption capacity with 5.3 and 4.2 mmol/g at 273 and 298 K respectively, which are among the best-reported values for carbon adsorbents derived from waste sources. Moreover, activated carbon material WDC-03 has high Isosteric heat of adsorption of (29.8–14.3KJ/mol). It has also shown excellent selectivity for CO_2 over N_2, with a value of ~16. Hence, Packaging waste is promising potential source for production of activated carbon with excellent carbon capture performance.

Acknowledgments

The authors acknowledge the financial support of NSF-AL-EPSCoR# 1655280, NSF-RISE #1459007, NSF-CREST#1137681, and NSF-MRI-1531934.

References

[1] U. Epa, C. Change Division, Inventory of U.S. Greenhouse Gas Emissions and Sinks: 1990-2015 – Executive Summary, (2017).
[2] IPCC, Climate Change 2014: Synthesis Report. Contribution of Working Groups I, II and III to the Fifth Assessment Report of the Intergovernmental Panel on Climate Change, (2014).
[3] P. Markewitz, et al., Worldwide innovations in the development of carbon capture technologies and the utilization of CO2, Energy Environ. Sci. 5 (May (6)) (2012) p. 7281.
[4] H. Yang, et al., Progress in carbon dioxide separation and capture: a review, J. Environ. Sci. 20 (January (1)) (2008) 14–27.
[5] C. Stewart, M.-A. Hessami, A study of methods of carbon dioxide capture and sequestration—the sustainability of a photosynthetic bioreactor approach, Energy Convers. Manag. 46 (February (3)) (2005) 403–420.
[6] J.C.M. Pires, F.G. Martins, M.C.M. Alvim-Ferraz, M. Simões, Recent developments on carbon capture and storage: an overview, Chem. Eng. Res. Des. 89 (September (9)) (2011) 1446–1460.
[7] Y.K. Salkuyeh, M. Mofarahi, Reduction of CO_2 capture plant energy requirement by selecting a suitable solvent and analyzing the operating parameters, Int. J. Energy Res. 37 (June (8)) (2013) 973–981.
[8] Sholeh Ma'mun, Roger Nilsen, H.F. Svendsen, O. Juliussen, Solubility of Carbon Dioxide in 30 Mass % Monoethanolamine and 50 Mass % Methyldiethanolamine Solutions, (2005).
[9] M. Hasib-ur-Rahman, F. Larachi, Prospects of using room-temperature ionic liquids as corrosion inhibitors in aqueous ethanolamine-based CO_2 capture solvents, Ind. Eng. Chem. Res. 52 (December (49)) (2013) 17682–17685.
[10] G. Li, P. Xiao, P. Webley, J. Zhang, R. Singh, M. Marshall, Capture of CO2 from high humidity flue gas by vacuum swing adsorption with zeolite 13X, Adsorption 14 (June (2–3)) (2008) 415–422.
[11] J.A. Mason, K. Sumida, Z.R. Herm, R. Krishna, J.R. Long, Evaluating metal–organic frameworks for post-combustion carbon dioxide capture via temperature swing adsorption, Energy Environ. Sci. 4 (August (8)) (2011) p. 3030.
[12] K.T. Leperi, R.Q. Snurr, F. You, Optimization of two-stage pressure/vacuum swing adsorption with variable dehydration level for postcombustion carbon capture, Ind. Eng. Chem. Res. 55 (March (12)) (2016) 3338–3350.
[13] A. Mittal, J. Mittal, A. Malviya, V.K. Gupta, Removal and recovery of chrysoidine Y from aqueous solutions by waste materials, J. Colloid Interface Sci. 344 (2) (2010) 497–507.
[14] V.K. Gupta, S. Agarwal, T.A. Saleh, Synthesis and characterization of alumina-coated carbon nanotubes and their application for lead removal, J. Hazard. Mater. 185 (1) (2011) 17–23.
[15] M. Ahmaruzzaman, V.K. Gupta, Rice husk and its ash as low-cost adsorbents in Water and wastewater treatment, Ind. Eng. Chem. Res. 50 (24) (2011) 13589–13613.
[16] N. Mohammadi, H. Khani, V.K. Gupta, E. Amereh, S. Agarwal, Adsorption process of methyl orange dye onto mesoporous carbon material-kinetic and thermodynamic studies, J. Colloid Interface Sci. 362 (2) (2011) 457–462.
[17] V.K. Gupta, A. Mittal, D. Jhare, J. Mittal, Batch and bulk removal of hazardous colouring agent Rose Bengal by adsorption techniques using bottom ash as adsorbent, RSC Adv. 2 (22) (2012) p. 8381.
[18] T.A. Saleh, V.K. Gupta, Column with CNT/magnesium oxide composite for lead(II) removal from water, Environ. Sci. Pollut. Res. 19 (4) (2012) 1224–1228.
[19] V.K. Gupta, A. Nayak, Cadmium removal and recovery from aqueous solutions by novel adsorbents prepared from orange peel and Fe2O3nanoparticles, Chem. Eng. J. 180 (2012) 81–90.
[20] V.K. Gupta, R. Kumar, A. Nayak, T.A. Saleh, M.A. Barakat, Adsorptive removal of dyes from aqueous solution onto carbon nanotubes: a review, Adv. Colloid Interface Sci. 193–194 (2013) 24–34.
[21] V.K. Gupta, T.A. Saleh, Sorption of pollutants by porous carbon, carbon nanotubes and fullerene—an overview, Environ. Sci. Pollut. Res. 20 (5) (2013) 2828–2843.
[22] T.A. Saleh, V.K. Gupta, Processing methods, characteristics and adsorption behavior of tire derived carbons: a review, Adv. Colloid Interface Sci. 211 (2014) 93–101.
[23] V.K. Gupta, A. Nayak, S. Agarwal, I. Tyagi, Potential of activated carbon from waste rubber tire for the adsorption of phenolics: effect of pre-treatment conditions, J. Colloid Interface Sci. 417 (2014) 420–430.
[24] I. Ali, Z.A. Al-Othman, A. Alwarthan, M. Asim, T.A. Khan, Removal of arsenic species from water by batch and column operations on bagasse fly ash, Environ. Sci. Pollut. Res. 21 (5) (2014) 3218–3229.
[25] M. Ghaedi, et al., Modeling of competitive ultrasonic assisted removal of the dyes - methylene blue and safranin-O using Fe3O4nanoparticles, Chem. Eng. J. 268 (2015) 28–37.
[26] I. Ali, Z.A. Alothman, M.M. Sanagi, Green synthesis of iron nano-impregnated adsorbent for fast removal of fluoride from water, J. Mol. Liq. 211 (2015) 457–465.
[27] I. Ali, Z.A. AL-Othman, A. Alwarthan, Molecular uptake of congo red dye from water on iron composite nano particles, J. Mol. Liq. 224 (2016) 171–176.
[28] D. Robati, et al., Removal of hazardous dyes-BR 12 and methyl orange using graphene oxide as an adsorbent from aqueous phase, Chem. Eng. J. 284 (2016) 687–697.
[29] A. Alonso, et al., Critical review of existing nanomaterial adsorbents to capture carbon dioxide and methane, Sci. Total Environ. 595 (2017) 51–62.
[30] G.-P. Hao, et al., Structurally designed synthesis of mechanically stable poly(benzoxazine-co-resol)-based porous carbon monoliths and their application as high-performance CO_2 capture sorbents, J. Am. Chem. Soc. 133 (29) (2011) 11378–11388.
[31] M.G. Plaza, A.S. González, C. Pevida, J.J. Pis, F. Rubiera, Valorisation of spent coffee grounds as CO2 adsorbents for postcombustion capture applications, Appl. Energy 99 (2012) 272–279.
[32] M. Sevilla, A.B. Fuertes, Sustainable porous carbons with a superior performance for CO2 capture, Energy Environ. Sci. 4 (5) (2011) p. 1765.
[33] M.A. Islam, I.A.W. Tan, A. Benhouria, M. Asif, B.H. Hameed, Mesoporous and adsorptive properties of palm date seed activated carbon prepared via sequential hydrothermal carbonization and sodium hydroxide activation, Chem. Eng. J. 270 (2015) 187–195.
[34] M.A. Lillo-Ródenas, J.P. Marco-Lozar, D. Cazorla-Amorós, A. Linares-Solano, Activated carbons prepared by pyrolysis of mixtures of carbon precursor/alkaline hydroxide, J. Anal. Appl. Pyrolysis 80 (1) (2007) 166–174.
[35] W. Sun, S.M. Lipka, C. Swartz, D. Williams, F. Yang, Hemp-derived activated carbons for supercapacitors, Carbon N. Y. 103 (2016) 181–192.
[36] T. Tay, S. Ucar, S. Karagöz, Preparation and characterization of activated carbon from waste biomass, J. Hazard. Mater. 165 (1–3) (2009) 481–485.
[37] D. Lozano-Castelló, M.A. Lillo-Ródenas, D. Cazorla-Amorós, A. Linares-Solano, Preparation of activated carbons from Spanish anthracite - I. Activation by KOH, Carbon N. Y. 39 (5) (2001) 741–749.
[38] A.C. Lua, T. Yang, Effect of activation temperature on the textural and chemical properties of potassium hydroxide activated carbon prepared from pistachio-nut shell, J. Colloid Interface Sci. 274 (2) (2004) 594–601.
[39] S.-M. Hong, E. Jang, A.D. Dysart, V.G. Pol, K.B. Lee, CO2 capture in the sustainable wheat-derived activated microporous carbon compartments, Sci. Rep. 6 (1) (2016) p. 34590.
[40] P.J.M. Carrott, P.A.M. Mourão, M.M.L.R. Carrott, Controlling the micropore size of activated carbons for the treatment of fuels and combustion gases, Appl. Surf. Sci. 252 (17) (2006) 5953–5956.
[41] A.S. Jalilov, et al., Asphalt-derived high surface area activated porous carbons for carbon dioxide capture, ACS Appl. Mater. Interfaces 7 (2) (2015) 1376–1382.
[42] G.P. Hao, W.C. Li, D. Qian, A.H. Lu, Rapid synthesis of nitrogen-doped porous carbon monolith for CO2 capture, Adv. Mater. 22 (7) (2010) 853–857.
[43] S. Deng, H. Wei, T. Chen, B. Wang, J. Huang, G. Yu, Superior CO2 adsorption on pine nut shell-derived activated carbons and the effective micropores at different temperatures, Chem. Eng. J. 253 (2014) 46–54.
[44] H. Wei, et al., Granular bamboo-derived activated carbon for high CO2 adsorption: the dominant role of narrow micropores, ChemSusChem 5 (12) (2012) 2354–2360.
[45] J. Serafin, U. Narkiewicz, A.W. Morawski, R.J. Wróbel, B. Michalkiewicz, Highly microporous activated carbons from biomass for CO2 capture and effective micropores at different conditions, J. CO2 Util. 18 (2017) 73–79.
[46] A.R. Mohamed, M. Mohammadi, G.N. Darzi, Preparation of carbon molecular sieve from lignocellulosic biomass: a review, Renew. Sustain. Energy Rev. 14 (6) (2010) 1591–1599.
[47] G. Davis, J.H. Song, Biodegradable packaging based on raw materials from crops and their impact on waste management, Ind. Crops Prod. 23 (2006) 147–161.
[48] A. Adrados, I. De Marco, B.M. Caballero, A. López, M.F. Laresgoiti, A. Torres, Pyrolysis of plastic packaging waste: a comparison of plastic residuals from material recovery facilities with simulated plastic waste, Waste Manag. 32 (5) (2012) 826–832.
[49] L. Li, R. Diederick, J.R.V. Flora, N.D. Berge, Hydrothermal carbonization of food waste and associated packaging materials for energy source generation, Waste

Manag. 33 (11) (2013) 2478–2492.
[50] F.A. López, T.A. Centeno, I. García-Díaz, F.J. Alguacil, Textural and fuel characteristics of the chars produced by the pyrolysis of waste wood, and the properties of activated carbons prepared from them, J. Anal. Appl. Pyrolysis 104 (2013) 551–558.
[51] J. Dlouhá, L. Suryanegara, H. Yano, The role of cellulose nanofibres in supercritical foaming of polylactic acid and their effect on the foam morphology, Soft Matter 8 (August (33)) (2012) p. 8704.
[52] L. Wang, et al., Corn starch-based graft copolymers prepared via ATRP at the molecular level, Polym. Chem. 6 (April (18)) (2015) 3480–3488.
[53] M. Thommes, et al., IUPAC technical report physisorption of gases, with special reference to the evaluation of surface area and pore size distribution (IUPAC technical report), Pure Appl. Chem. (2015).
[54] A. Shahtalebi, A.H. Farmahini, P. Shukla, S.K. Bhatia, Slow diffusion of methane in ultra-micropores of silicon carbide-derived carbon, Carbon N. Y. 77 (2014) 560–576.
[55] H. Wei, et al., Excellent electrochemical properties and large CO2 capture of nitrogen-doped activated porous carbon synthesised from waste longan shells, Electrochim. Acta 231 (2017) 403–411.
[56] Y. Sha, J. Lou, S. Bai, D. Wu, B. Liu, Y. Ling, Facile preparation of nitrogen-doped porous carbon from waste tobacco by a simple pre-treatment process and their application in electrochemical capacitor and CO2 capture, Mater. Res. Bull. 64 (2015) 327–332.
[57] Y. Boyjoo, et al., From waste Coca Cola® to activated carbons with impressive capabilities for CO2 adsorption and supercapacitors, Carbon N. Y. 116 (2017) 490–499.
[58] G.K. Parshetti, S. Chowdhury, R. Balasubramanian, Biomass derived low-cost microporous adsorbents for efficient CO2 capture, Fuel 148 (2015) 246–254.
[59] J. Choma, M. Marszewski, L. Osuchowski, J. Jagiello, A. Dziura, M. Jaroniec, Adsorption properties of activated carbons prepared from waste CDs and DVDs, ACS Sustain. Chem. Eng. 3 (4) (2015) 733–742.
[60] S. García, M.V. Gil, C.F. Martín, J.J. Pis, F. Rubiera, C. Pevida, Breakthrough adsorption study of a commercial activated carbon for pre-combustion CO2 capture, Chem. Eng. J. 171 (2) (2011) 549–556.